Structure and Function of *S*-Adenosylmethionine Synthetase: Crystal Structures of *S*-Adenosylmethionine Synthetase with ADP, BrADP, and PP_i at 2.8 Å Resolution[†,‡]

Fusao Takusagawa,*[,§] Shigehiro Kamitori,[§] and George D. Markham[||]

Departments of Chemistry and Biochemistry, University of Kansas, Lawrence, Kansas 66045-0046, and The Institute for Cancer Research, The Fox Chase Cancer Center, Philadelphia, Pennsylvania 19111

Received November 2, 1995; Revised Manuscript Received December 20, 1995[⊗]

ABSTRACT: *S*-Adenosylmethionine synthetase (MAT, ATP:L-methionine *S*-adenosyltransferase, EC 2.5.1.6) plays a central metabolic role in all organisms. MAT catalyzes the two-step reaction which synthesizes *S*-adenosylmethionine (AdoMet), pyrophosphate (PP_i), and orthophosphate (P_i) from ATP and L-methionine. AdoMet is the primary methyl group donor in biological systems. The first crystal structure of MAT from *Escherichia coli* has recently been determined [Takusagawa *et al*. (1995) *J. Biol. Chem. 271*, 136−147]. In order to elucidate the active site and possible catalytic reaction mechanism, the MAT structures in the crystals grown with the substrate ATP (and BrATP) and the product PP_i have been determined (space group $P6_222$; unit cell $a = b = 128.9$ Å, $c = 139.8$ Å, resolution limit 2.8 Å; R 0.19; R_{free} 0.26). The enzyme consists of four identical subunits; two subunits form a spherical dimer, and pairs of these tightly bound dimers form a tetrameric enzyme. Each dimer has two active sites which are located between the subunits. Each subunit consists of three domains related to each other by a pseudo 3-fold symmetry. The crystal structures showed that the ATP molecules were hydrolyzed to ADP and P_i by the enzyme. Those products were found at the active site along with the essential metal ions (K^+ and Mg^{2+}). This rather unexpected finding was first confirmed by the structure of the complex with PP_i and later by an HPLC analysis. The enzyme hydrolyzed ATP to ADP and P_i in 72 h under the same conditions as the crystallization of the enzyme. In the active site, the diphosphate moiety of ADP and P_i interacts extensively with the amino acid residues from the two subunits of the enzyme, whereas the adenine and ribose moieties have little interaction with the enzyme. The enzyme structure is little changed upon binding ADP. All amino acid residues involved in the active site are found to be conserved in the 14 reported sequences of MAT from a wide range of organisms. Thus the structure determined in this study can be utilized as a model for other members of the MAT family. On the basis of the crystal structures, the catalytic reaction mechanisms of AdoMet formation and hydrolysis of tripolyphosphate are proposed.

In biological systems, there are a myriad of reactions in which methyl groups are transferred from a few types of methyl donors to a wide variety of methyl acceptors. Among biological methyl group donors, *S*-adenosylmethionine (AdoMet),[1] discovered by Cantoni in 1953, is the most widely used, while 5-methyltetrahydrofolic acid, methylcobalamine, and betaine are involved in far fewer methylation reactions.

The formation of AdoMet is catalyzed solely by AdoMet synthetase (MAT, ATP:L-methionine *S*-adenosyltransferase, EC 2.5.1.6) and occurs in an unusual two-step reaction in which the complete triphosphate chain is cleaved from ATP as AdoMet is formed, and the tripolyphosphate is further hydrolyzed to PP_i and P_i before the sulfonium product (AdoMet) is released, giving the overall reaction shown in Scheme 1 (Mudd & Cantoni, 1958). Thus the enzyme must catalyze reactions at both ends of the triphosphate chain which appears to be a unique catalytic task. This quite unusual catalytic reaction has been studied by various methods. The AdoMet-forming reaction was found by stereochemical and kinetic isotope studies to occur as an S_N2 reaction with direct attack of the sulfur of methionine on

Scheme 1

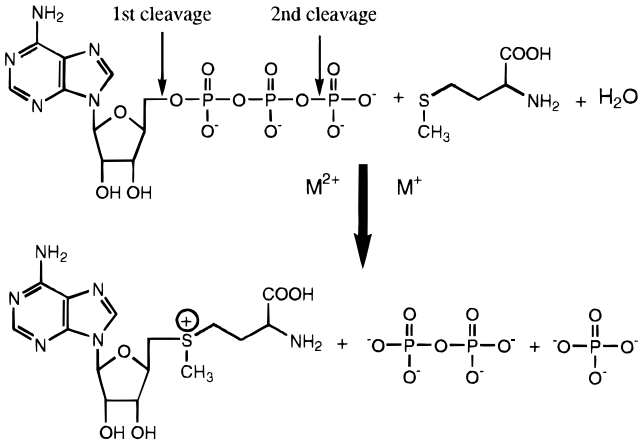

† The work carried out at the University of Kansas has been supported by NIH Grant GM37233 and in part by the Kansas Health Foundation and the Marion Merrell Dow Foundation. The work carried out at The Fox Chase Cancer Center has been supported by the NIH Grants GM31186, CA06927, and RR05539 and by an appropriation from the Commonwealth of Pennsylvania.

‡ The atomic coordinates have been deposited with the Brookhaven Protein Data Bank (entry names 1MXA, 1MXB, and 1MXC).

* Author to whom all correspondence should be addressed.

§ University of Kansas.

|| The Fox Chase Cancer Center.

⊗ Abstract published in *Advance ACS Abstracts,* February 1, 1996.

[1] Abbreviations: AdoMet, *S*-adenosylmethionine; BrAPT, 8-BrADP; P_i, orthophosphate; PP_i, pyrophosphate; MAT, ATP:L-methionine *S*-adenosyltransferase; MAT−ADP, MAT complexed with ADP; MAT−BrADP, MAT complexed with BrADP; MAT−P_i, MAT complexed with P_i; MAT−PP_i, MAT complexed with PP_i.

Table 1: Experimental Details and Refinement Parameters[a]

data set	MAT−PP_i	MAT−ADP	MAT−BrADP
source of data[b]	MARK-III	MARK-III	DIP100S
resolution (Å)	10−2.8	10−2.8	10−3.0
no. of crystals	27	6	2
no. of reflections measured	229007	51217	56509
no. of unique reflections	16991	16033	13244
% complete	100.0	94.4	95.8
R_{sym}[c]	0.074	0.053	0.069
	Refinement Parameters		
no. of residues	377	377	377
contents of ions	PP_i, P_i, 2Mg, 2K	ADP, P_i, 2Mg, 2K	BrADP, P_i, 2Mg, 2K
no. of atoms	2917	2934	2935
R[d]	0.190	0.194	0.187
RMS deviations			
bond (Å)	0.014	0.014	0.015
angle (deg)	3.3	3.4	3.4
torsion angle (deg)	25.5	26.0	25.7
mean *B* values			
Cα	28.7	27.9	29.0
main chain	29.6	28.7	29.8
all atoms	32.4	31.8	32.7

[a] Space group $P6_222$; cell dimensions (Å) $a = b = 128.9$, $c = 139.8$; number of amino acid residues 383; M_r of subunit 42 000; percentage of solvent content 63%. [b] MARK-III: the diffraction data were measured at the University of California at San Diego using the MARK-III multiwire area detractor X-ray diffractometer. DIP100S: the diffraction data were measured at the University of Kansas using a DIP100S imaging plate X-ray diffractometer. [c] $R_{sym} = \sum|\langle I\rangle - I|/\sum\langle I\rangle$. [d] $R = \sum|F_o - F_c|/\sum F_o$.

the C5′ atom of ATP (Parry & Minta, 1982; Markham *et al*., 1987). Cantoni originally reported that divalent metals are essential for activity (Cantoni, 1953). EPR spectroscopic studies suggested the presence of two divalent metal ions in the active site (Markham, 1981; Zhang *et al*., 1993). Indeed, two divalent metal binding sites have been found by the previous X-ray study on the complex with two P_i's (Takusagawa *et al*., 1995). The enzymatic mechanism has been studied by using numerous ATP and methionine analogues which have inhibitory activity against the enzyme (Sufrin *et al*., 1981, 1993; Ma *et al*., 1990). An ATP binding region has been proposed on the basis of the sequences of the *Escherichia coli* enzyme (Markham & Satishchandran, 1988) and the liver enzyme (Horikawa *et al*., 1989).

The determination of the three-dimensional structures of the enzyme with the bound substrates is essential to elucidate the unique catalytic mechanism, as well as to facilitate development of effective inhibitors for this enzyme. Three X-ray structures showing MAT after hydrolysis of ATP will be described in this paper.

EXPERIMENTAL PROCEDURES

Crystallization. The crystals of the pyrophosphate complex (MAT−PP_i) were grown from a solution containing 100 mM potassium phosphate (pH 7.0), 10 mM $Na_4P_2O_7$, 10 mM $MgCl_2$, and 33% (v/v) saturated ammonium sulfate with the protein concentration at 10 mg/mL. The hexagonal bipyramidal shaped crystals were grown at 26 °C for 2 weeks. The crystals belonged to the hexagonal crystal system with the space group $P6_222$. The crystals of the ADP complex (MAT−ADP) were obtained from the same solution as for the MAT−PP_i complex except for containing 10 mM ATP instead of $Na_4P_2O_7$. The crystals of the BrADP complex (MAT−BrADP) were prepared by a soaking method. First, the native crystals (MAT−P_i) were grown from a solution containing 100 mM potassium phosphate (pH 7.0), 10 mM $MgCl_2$, and 33% (v/v) saturated ammonium sulfate with the protein concentration at 10 mg/mL, and then the mother liquor of the native crystals was gradually replaced with the artificial mother liquor containing 50 mM BrATP in 50 mM Tris-HCl buffer (pH 7.5), 50 mM $MgCl_2$, and 35% (v/v) saturated ammonium sulfate for 3 days at 26 °C.

Data Measurement. As the crystals decayed very quickly under X-ray exposure conditions required for data collection, the diffraction data were obtained by using several fresh crystals. The 2.8 Å resolution data for the MAT−PP_i and MAT−ADP complexes were measured on the MARK-III multiwire area detector X-ray diffractometer (Xuong *et al*., 1985), while the 3.0 Å resolution data for MAT−BrADP were measured on a locally modified DIP100S imaging plate X-ray diffractometer (MAC Science); Cu Kα radiation was used in both cases. The diffraction data of the MAT−BrADP complex were processed with the program ELMS (Tanaka *et al*., 1990), whereas the data of the MAT−PP_i and MAT−ADP complexes were processed by the software associated with MARK-III (Xuong *et al*., 1985). Integrated reflections of the complexes were scaled and reduced with the locally developed programs (Takusagawa, 1992). The data statistics are given in Table 1.

Structure Determination of PP_i Complex. The structure of MAT in the MAT−PP_i complex was initially refined with the coordinates of the protein structure of MAT−P_i (Takusagawa *et al*., 1995). The difference map calculated with coefficients of $(F_o - F_c)$ and calculated phases showed significant residual electron density peaks in the region of active sites (Figure 2). The electron density peaks of the MAT−PP_i complex were assigned to the PP_i and P_i moieties and K^+ and two Mg^{2+} ions on the basis of the size of the electron density peak, refined temperature factors, and polar environment, and those ions were introduced into refinement. An additional residual electron density peak found near the center of the tightly bound dimer and on the 2-fold axis was significant as observed in the MAT−P_i structure and was assigned to the K^+ ion on the basis of the size of the electron density peak and polar environment. The initial models were built on an IRIS workstation using the program TOM/

FRODO (Jones, 1985; Cambillau & Horjales, 1987) and were refined with the positional protocol and then the simulated annealing procedure of X-PLOR (Brünger, 1993). Refinement of the isotropic temperature factor for individual atoms was carried out by the individual *B*-factor refinement procedure of X-PLOR using bond (1−2) and angle (1−3) restraints. Residues 102−107, which are outside the active site, were not visible in the electron density maps and were assumed to be heavily disordered. Although those residues were arbitrarily traced using a TOM/FRODO routine (Jones, 1985; Cambillau & Horjales, 1987), those residues were not included in the refinement. No water molecule was included in refinements. The parameters of structure determination and refinement are listed in Table 1.

Structure Determinations of ADP and BrADP Complexes. After 30 cycles of positional refinement of the protein structure in the MAT−ADP complex, the difference map calculated with coefficients ($F_o - F_c$) and the protein phases of MAT showed residual electron density peaks similar to those observed in the MAT−PP_i complex described above (Figure 2). The difference map of the BrADP complex also showed the similar residual electron density peaks as observed in the ADP complex (Figure 2). These residual electron density peaks indicated that the ATP molecule was hydrolyzed to ADP and P_i. This was confirmed by the HPLC analyses as described below. In addition to those phosphate electron density peaks, a large, flat and elongated electron density peak apparently due to the adenine ring was observed in the active site. The electron density peak for the Br atom in the BrADP complex was significantly high in the one end of the adenine ring, clearly indicating the orientation of the adenine ring. Although the electron density peak for the ribose moiety which should be located between the phosphate and adenine moieties was relatively weak, the well-defined electron density peaks of the diphosphate moiety and the adenine ring allowed building of a model of ADP and BrADP into the density map without any ambiguity. The initial models were built on an IRIS workstation using the program TOM/FRODO (Jones, 1985; Cambillau & Horjales, 1987) and were refined with the positional protocol and then the simulated annealing procedure of X-PLOR (Brünger, 1993). The models were rebuilt where necessary. The structures were refined by the same procedures applied for the structure refinement of the MAT−PP_i complex.

Measurement of ATP Hydrolysis to ADP. A solution used for MAT−ADP crystallization, which is composed of 100 mM potassium phosphate (pH 7.0), 10 mM $MgCl_2$, 33% (v/v) saturated ammonium sulfate, and 10 mM ATP, was prepared. The MAT solution (20 mg/mL protein concentration) was mixed with an equal volume of the crystallization solution. After centrifugation for 5 min, the mixture was separated into two microcentrifuge tubes. One tube was kept in a 26 °C incubator, and the other tube was put in a −135 °C freezer. A portion of the crystallization buffer was also kept in a 26 °C incubator. After 72 h, the contents of three tubes were analyzed by HPLC using a 10 mm × 25 cm C18 reverse-phase column (Rainin Dynamax-300A). The conditions were as follows: buffer A, 200 mM potassium phosphate (pH 7.0); buffer B, acetonitrile; gradient, 0−30% B in 20 min; flow, 2.5 mL/min; temperature, 23 °C. The absorbance at 260 nm was recorded. A mixture of ATP and ADP was also recorded using the same conditions for a reference. The mixture kept in −135 °C freezer and the crystallization solution containing ATP gave a major peak at the same retention time as ATP, suggesting no hydrolysis of the ATP molecule, whereas a major peak from the mixture kept in the 26 °C incubator was approximately 2 min later than ATP and agreed with the retention time of ADP, indicating the conversion of ATP to ADP (Figure 4).

RESULTS AND DISCUSSION

Overall Structure. The overall structures of MAT complexed with PP_i, ADP, and BrADP are essentially the same as the structure of the MAT−P_i complex (Takusagawa *et al.*, 1995). The maximum root-mean-square deviation of the Cα atoms from the MAT−P_i structure is less than 0.30 Å for all three complex structures. MAT consists of four identical subunits related by 222 symmetry. Pairs of subunits strongly interact with each other to form a spherical dimer, and these dimers associate to a tetrameric enzyme. Each dimer has two active sites located between subunits, with amino acid residues from both subunits contributing to each active site. In this paper, amino acid residues in the second subunit are indicated with an asterisk, such as His^{14*}. The three domains denoted the N-terminal domain (residues 1−12, 129−233), the central domain (residues 13−101, 234−268), and the C-terminal domain (residues 108−128, 269−383) are related to each other by a pseudo-3-fold symmetry (Figure 1).

Pyrophosphate Binding. In the MAT−PP_i complex, a difference map calculated after 30 cycles of positional refinement of the protein structure showed the significant residual electron density peaks in the active site (Figure 2). The PP_i, P_i, K^+, and two Mg^{2+} ions were fitted into the residual electron density map. Although the electron density distribution is somewhat similar to that of the MAT−P_i complex (Takusagawa *et al.*, 1995), there are clearly differences between PP_i and P_i complexes. The P_i, K^+, and two Mg^{2+} ions are located at the same positions of those ions in the MAT−P_i structure (Takusagawa *et al.*, 1995). One of the phosphates of the PP_i is approximately located at the second P_i position of the MAT−P_i structure.

Possible interactions between amino acid residues and the PP_i, P_i, and metal ions are illustrated in Figure 3A. His^{14*}(Nε2) and Lys^{165*}(Nζ) bind with hydrogen bonds to one of the phosphoryl groups of PP_i, which corresponds to the β-phosphoryl group of ADP, whereas Lys^{265}(Nζ), Arg^{244*}(Nε), and Lys^{245*}(Nζ) participate in hydrogen bonds to the P_i ion. Interactions between these positively charged residues and the negatively charged oxygen atoms of the PP_i and P_i ions appear to neutralize the individual charges. Some of these positively charged residues might be involved in the hydrolysis of tripolyphosphate to PP_i and P_i.

Two Mg^{2+} ions separated by 5 Å bridge PP_i and P_i ions in a pyramidal fashion; *i.e.*, each Mg^{2+} ion is coordinated by two oxygen atoms of the PP_i ion and one oxygen atom of the P_i ion. The negatively charged Asp^{271} and Asp^{16*} residues coordinate the two Mg^{2+} ions, respectively, from the opposite side of the phosphate ions (PP_i and P_i). Similar polar interactions are found in the ADP and BrADP complexes as will be described below.

ATP Binding. Both ATP and BrATP are good substrates for MAT with comparable K_M values, and BrATP has one-third of the maximal catalytic rate with ATP (Markham *et al.*, 1980). The Br atom in the BrATP is quite helpful in

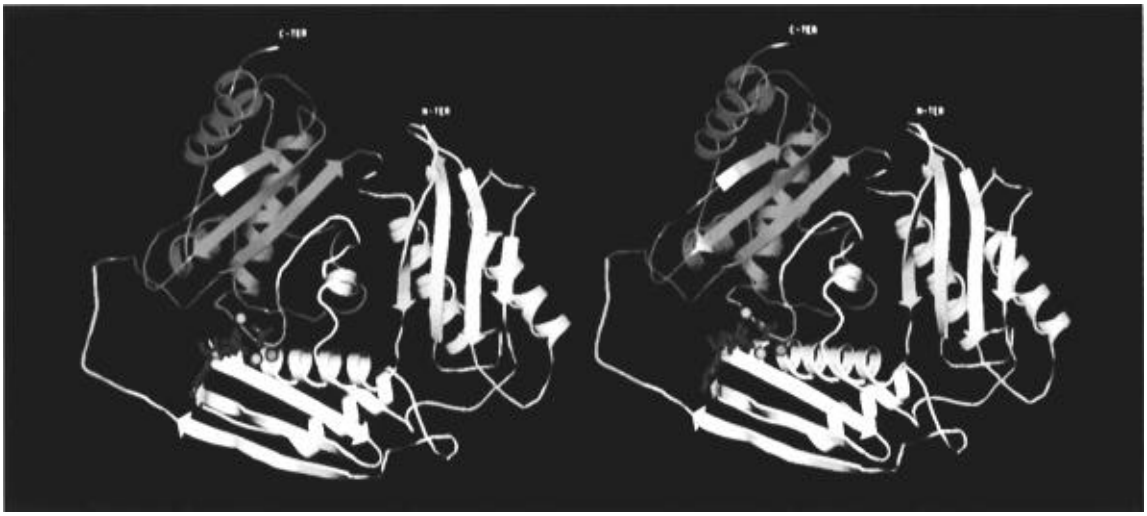

FIGURE 1: Ribbon drawing of a subunit of MAT showing three domains [*N*-terminal domain (yellow), central domain (white), and C-terminal domain (green)]. ADP (red), P_i (red), two Mg^{2+} ions (orange), and one K^+ (magenta) ion are superimposed. The P-loop-like region is colored with magenta, whereas the "flexible loop" built arbitrarily is indicated by light blue.

determining the position and orientation of the molecule bound to the enzyme. Thus, structures of the complexes with ATP and BrATP were determined in order to assure the position and orientation of ATP in the active site. ATP was cocrystallized with MAT whereas BrATP was soaked into the native MAT crystals. Although the crystals of MAT−ADP and MAT−BrADP were differently prepared, both ATP and BrATP were found to be hydrolyzed to ADP and BrADP, respectively. As will be discussed below, this result eliminates a possible hydrolysis activity by a small amount of ATPase contamination in the enzyme solution.

A difference map of the MAT−ADP complex calculated after 30 cycles of positional refinement of the protein structure showed significant residual electron density peaks in the active site. An elongated flat electron density peak was located at the entrance of the active site, which apparently corresponded to the adenine ring moiety of ATP. The electron density peak for the ribose moiety was relatively weak and did not show up at the 3σ contour level, suggesting that the ring took multiple conformations (Figure 2). Surprisingly, the residual electron density peaks in the triphosphate binding region were identical to those of the PP_i complex which contained PP_i, P_i, K^+, and two Mg^{2+} ions in the active site as described above, suggesting that ATP was hydrolyzed to ADP and the P_i ion. Thus, the ADP molecule and P_i ion were fitted into the residual electron density map along with K^+ and two Mg^{2+} ions, and the model was refined successfully. Similar residual electron density distribution was observed in the difference map of the MAT−BrADP complex, except for distinguishably high electron density peak at the Br atom, indicating the orientation of the adenine ring. The hydrolysis has been confirmed by a simple HPLC analysis (Figure 4). The MAT enzyme indeed hydrolyzed completely ATP to ADP in 72 h under the same conditions used for preparation of the complex crystals of MAT−ADP. ATP was not hydrolyzed to ADP without the enzyme under the same conditions. Hydrolysis of MAT catalyzed ATP to ADP and P_i was previously reported to occur at ~0.1% of the rate of AdoMet formation under vastly different conditions (Markham *et al.*, 1980).

The dissociation constant for ADP binding to MAT is >100 times larger than that of ATP (Markham *et al.*, 1980). Thus, if ATP was hydrolyzed by a small amount of ATPase contamination in the enzyme, then the structures of the active sites in the MAT−ADP and MAT−BrADP complexes would be different from each other since the crystals of two complexes were prepared quite differently. The crystals of MAT−ADP were prepared by the cocrystallization method for 2 weeks. The ATP molecules would be completely hydrolyzed by the contaminated ATPase into ADP before MAT crystallized as the MAT−ADP complex. Thus, ADP might cocrystallize with MAT. On the other hand, since crystals of the MAT−BrADP complex were prepared by soaking crystals with excess ATP (50 mM) and since ATP binds to MAT much stronger than ADP, ATP should be in the active site if MAT did not hydrolyze ATP by itself. Thus, the observed ATPase activity is due to MAT but not to a contamination. This ATPase activity of MAT has little been investigated, and thus its biological role is unknown. However, since the ATPase activity of MAT is a very slow process in comparison with the AdoMet formation and furthermore MAT does not produce AdoMet from ADP and L-methionine, the ATPase activity is probably not an important event in biological systems.

The interactions of the diphosphate moiety of ADP and the P_i ion with amino acid residues are shown in Figure 3B. Similar interactions were found in the MAT−BrADP complex. The polar interactions of the phosphate groups in the active site are identical to those found in the MAT−PP_i complex described above. The diphosphate moiety and the P_i ion interact strongly with the enzyme, whereas the adenine and ribose moieties have little interaction with the enzyme.

The electron density peaks of the adenine base and ribose moieties are relatively weak in comparison to that of the diphosphate moiety and the P_i ion. Indeed, these moieties have relatively large thermal motions, suggesting that they bind weakly to the enzyme. The adenine ring is located on the hydrophobic β-sheet which consists of three β-strands (B2, B3, and B4) of the central domain (Figure 1). Although N3 of the adenine ring is involved in a hydrogen bond with $Lys^{269}(N\zeta)$, the adenine ring appears to be recognized by forming a hydrogen bond with its N6 amino group to the carbonyl oxygen Oϵ1 of Gln^{98} which is the only hydrogen bond acceptor on the surface of the adenine pocket. The

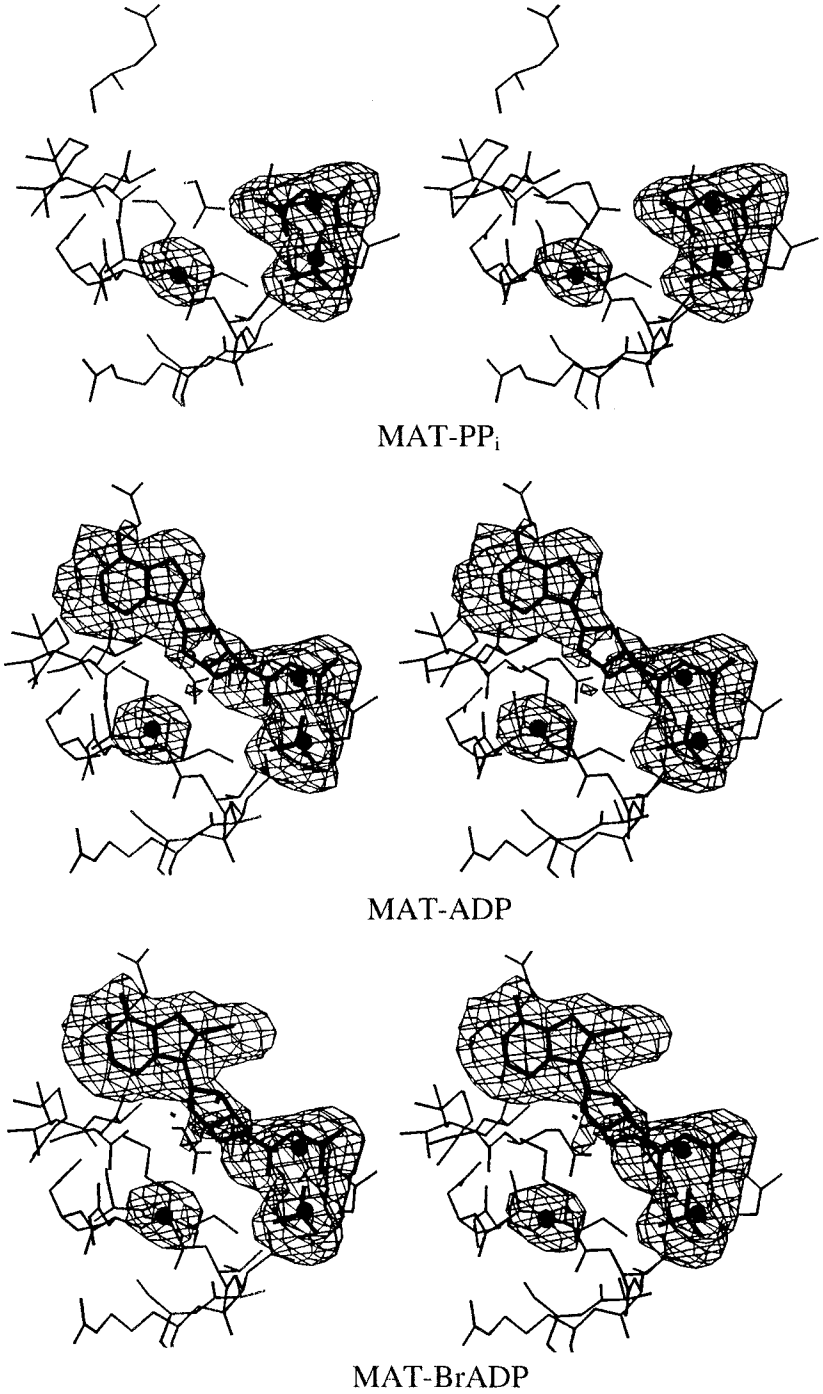

FIGURE 2: Difference electron density maps (omit maps) calculated after 30 cycles of the positional refinement of the protein structure by X-PLOR. The contours are drawn at a 1.75σ level. The final model is superimposed in the map. The Mg^{2+} ions (●) are associated with the phosphate groups in the center of the maps. The electron density peak of the K^+ ion (●) is on the left side of the maps.

amino acid residues constituting the adenine pocket are tightly connected to each other by hydrogen bonds. For example, Gln^{98}(Nϵ2) is linked to Gly^{96}(O) and Glu^{55}(Oϵ1), and Glu^{55}(Oϵ2) is connected to Lys^{46*}(Nζ), which in turn is linked to Gly^{54}(O) and Ala^{94}(O) by hydrogen bonds. This hydrogen bond network prevents rotation around the Cγ−Cδ bond of Gln^{98}, preventing the Nϵ2 group of Gln^{98} from being present in the adenine pocket. If the amino group (Nϵ2) of Gln^{98}, a hydrogen bond donor, were on the surface, then a guanine might be recognized instead of adenine through formation of a hydrogen bond between Nϵ2 of Gln^{98} and O4 of guanine. It should be noted that GTP is neither a substrate nor a good inhibitor (Markham *et al.*, 1980).

The electron density peaks of the ribose moieties in both MAT−ADP and MAT−BrADP complexes are relatively weak, suggesting that the ribose takes multiple ring conformations. Probably for this reason, no distinguishable hydrogen bonds between the ribose moiety and the amino acid residues are found in the structure. However, the O2′ and O3′ hydroxyl groups of the ribose are surrounded within 4.5 Å by hydrophilic groups, Gly^{117}(O) (4.5 Å), and Asp^{118}(Oδ2) (3.9 Å). These amino acid residues might participate in hydrogen bonding to the hydroxyl groups through disordered water molecules. As described above, in comparison with the phosphate moiety, the adenine and ribose moieties do not interact strongly with the enzyme.

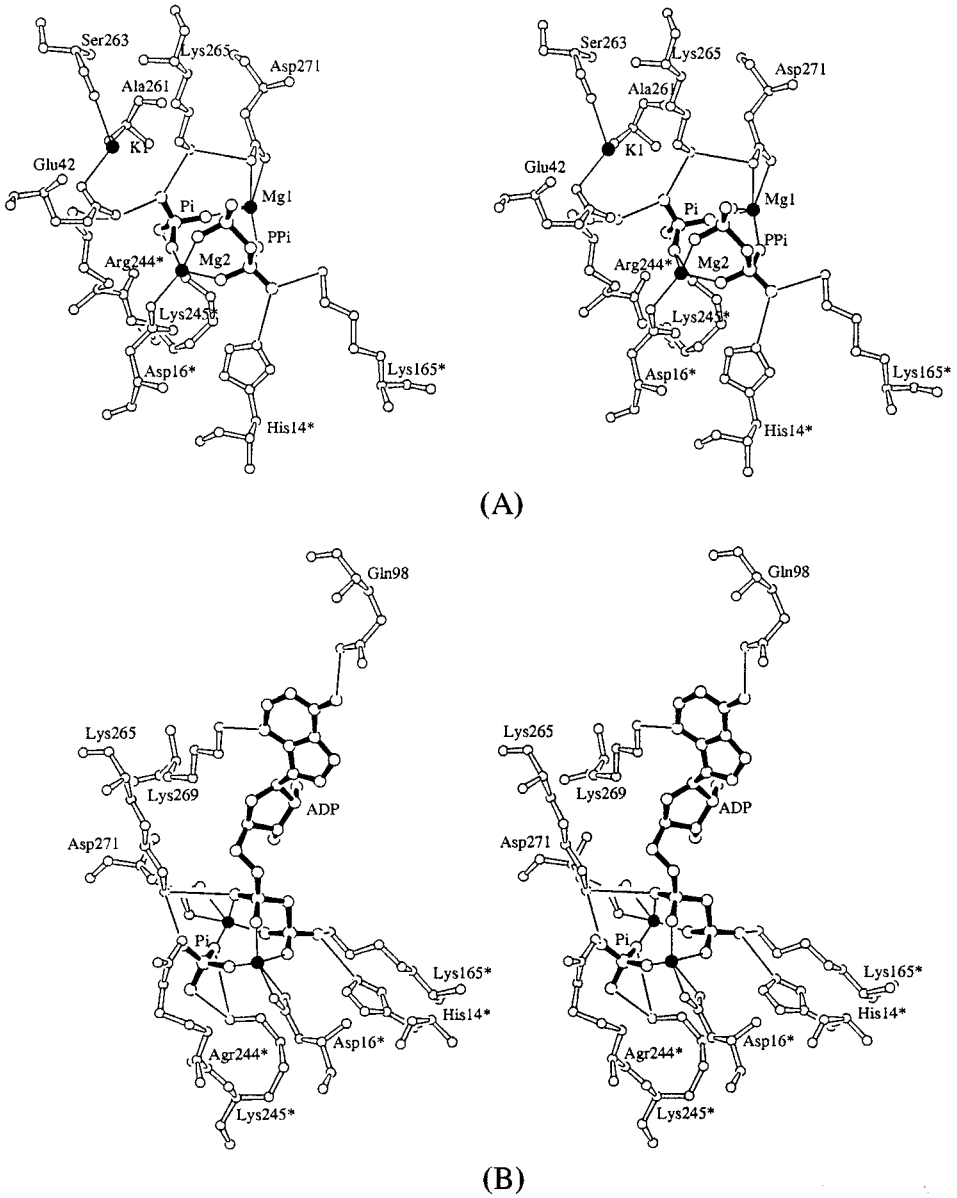

FIGURE 3: Active site geometry with (A) PP_i, P_i, Mg^{2+}, and K^+ ions and with (B) ADP, P_i, Mg^{2+}, and K^+ ions. Possible polar interactions (hydrogen and coordinate bonds) are indicated by thin lines. The PP_i, P_i, and ADP are illustrated by the solid bonds while the metal ions are shown by the filled circles. The hydrogen and coordination bonds are defined as donor−acceptor distances less than 3.3 Å and metal−oxygen distances less than 2.5 Å, respectively.

This weak interaction may facilitate the release of the product (AdoMet) from the active site after the catalytic reaction. It should be noted that since the electron density peaks of ribose moieties in both MAT−ADP and MAT−BrADP are very weak, the data cannot completely exclude a possibility of the presence of PP_i and adenine in the active site rather than ADP; however, this would be inconsistent with the HPLC analyses.

P-Loop-like Sequence in ATP Binding Region. Many ATP/GTP binding proteins have a triphosphate binding loop (P-loop) with the consensus glycine-rich sequence of GXXXXGK[S/T] (Saraste *et al.*, 1990). For example, a typical P-loop found in the structure of *ras p*21 protein consists of a β-turn with four residues (Ala^{11}-Gly^{12}-Gly^{13}-Val^{14}) between the conserved glycine residue (Gly^{10}) and GK[S/T] (Gly^{15}-Lys^{16}-Ser^{17}). The loop is located between a β-strand and an α-helix (Pai *et al.*, 1989). The triphosphate moiety of the GTP analogue, guanosine 5′-(β,γ-imido)-triphosphate (GppNp), is enveloped by the P-loop residues, and several amido hydrogen atoms of the P-loop residues point toward the triphosphate moiety so as to neutralize the charge. The conserved Lys^{16}(Nζ) participates in a hydrogen bond with the triphosphate moiety of the GppNp and also to the main-chain oxygen atoms of Gly^{10} and Ala^{11}. The conserved Ser^{17} residue coordinates the Mg^{2+} ion which is also coordinated by the triphosphate moiety.

A P-loop-like sequence has been found in the MAT sequence around the ATP binding region (Figure 1). The sequence from 259 to 266, GGAFSGKD, fits the P-loop sequence criteria GXXXXGK[S/T] described above, except for the serine/threonine [S/T] residue which is replaced by an aspartate [D]. However, the three-dimensional structure of the P-loop-like sequence found in the MAT structure is completely different from those of the typical P-loops described above. Lys^{265} is the only conserved amino acid residue in the P-loop-like sequence which participates in a polar interaction (hydrogen bond) with the P_i ion (Figure 3B). Most of the amino acid residues in the P-loop-like

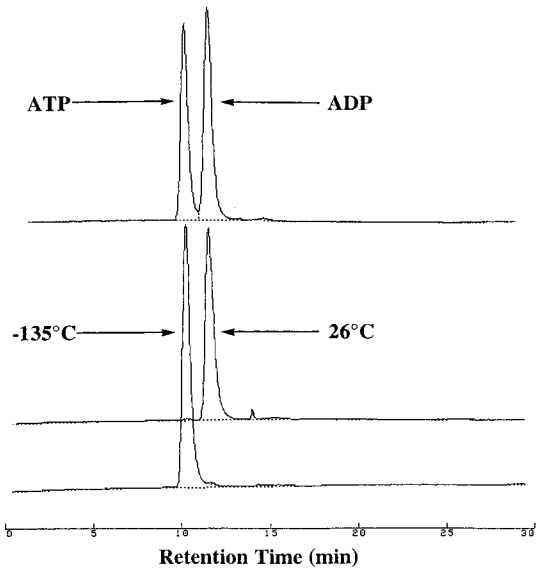

FIGURE 4: HPLC analysis of the ATPase reaction as catalyzed by MAT. The chromatographs of the sample kept in a −135 °C freezer and the sample incubated at 26 °C for 72 h are marked with "−135 °C" and "26 °C", respectively. The chromatograph of the mixture of ATP and ADP is superimposed for reference.

sequence are located relatively far from the P_i and PP_i moiety. Furthermore, the vicinity of the loop is quite different from the region of the typical P-loop. There are two consecutive β-turns in the P-loop-like sequence region of MAT, instead of the one turn in the typical P-loop. The first β-turn consists of four residues (Phe^{262}-Ser^{263}-Gly^{264}-Lys^{265}) including the conserved lysine residue (Lys^{265}), and the second β-turn consists of four successive residues (Asp^{266}-Pro^{267}-Ser^{268}-Lys^{269}). Lys^{265}(Nζ) participates in a hydrogen bond with the main-chain oxygen atom of the preceding residue (Ala^{261}) in the first β-turn loop, and another lysine residue, Lys^{269}(Nζ), hydrogen bonds to the Oδ1 atom of the preceding residue (Asp^{266}) in the second β-turn loop. As a result, each β-turn loop consists of four or five residues which form a cyclic structure closed by the hydrogen bond of the lysine side chain, *i.e.*, Ala^{261}•••Lys^{265} and Asp^{266}•••Lys^{269} (Figure 5). Interestingly, both of the cyclic structures are composed of 18 atoms. Furthermore, Lys^{265} in the first cyclic loop is located near the P_i ion (γ-phosphoryl group) while Lys^{269} in the second loop is near the ribose moiety. More specifically, Lys^{265} in the first β-turn involves in a hydrogen bond with the P_i ion whereas Lys^{269} in the second β-turn can participate in a hydrogen bond with O5′ by changing the torsion angles of the side chain. It should be noted that most ATP/GTP binding enzymes catalyze cleavage of one high-energy phosphoryl bond. On the other hand, MAT cleaves not only the γ-phosphoryl group from the triphosphate moiety but also the C5′−O5′ bond of ATP. Thus, these two rather unusual consecutive 18-member loops might be involved catalysis of the two bond cleavage events. As will be described below, the Lys^{265} in the first loop appears to participate in the hydrolysis of the triphosphate chain of ATP, and the Lys^{269} in the second loop might play an important role of cleavage of the C5′−O5′ bond by transferring a proton of the amino group (Nζ) to the O5′ oxygen.

Roles of Active Site Residues. The interactions of ADP, P_i, metal ions, and amino acid residues are summarized in Figure 6. The residues which interact directly with ADP, P_i, and metal ions are likely to be functionally important residues. As will be described below, all these residues are found to be conserved in the 14 reported AdoMet synthetase sequences from a wide range of organisms.

In the reaction catalyzed by MAT, synthesis of AdoMet and tripolyphosphate from ATP and L-methionine is followed by cleavage of tripolyphosphate to PP_i and P_i. This hydrolysis occurs between β- and γ-phosphates with the water oxygen being incorporated into the P_i formation (Mudd & Cantoni, 1958; Markham *et al.*, 1980). This study confirms the hydrolysis occurred between the β- and γ- phosphates of tripolyphosphate since ATP was found to be hydrolyzed to ADP and P_i in the active site of MAT. The bridging Mg^{2+} ions appear to be involved in the catalytic reactions at both ends of the triphosphate chain. The Mg^{2+} coordination found in this study is quite consistent with the previous studies. Specifically, MAT requires the mono- and divalent ions to produce AdoMet not only from ATP and L-methionine but also from AMPPNP and L-methionine. The mono- and divalent ions are required for maximal rate of hydrolysis of the tripolyphosphate to PP_i and P_i (Markham *et al.*, 1980). The carboxyl groups of Asp^{271} and Asp^{16*} which coordinate the Mg^{2+} ions appear to hold these important metal ions. The side chain of Glu^{42} coordinates the K^+ ion as does the carbonyl of Ser^{263}. Glu^{42} also forms a strong salt bridge with Arg^{244*}. Since no direct interaction between the K^+ ion and ADP (BrADP) or P_i is seen in the structure, the main role of the K^+ ion might be to organize the structure of the active site, a situation analogous to that recently found for K^+ ion in pyruvate kinase (Larsen *et al.*, 1994). The other monovalent ion, which is assumed to be a K^+ ion, located at center of the dimer might be important to construct the tightly bound dimer structure (see Figure 7).

In all organisms studied so far, multiple forms of MAT have been found. The amino acid sequences of the enzyme from *E. coli* (Markham *et al.*, 1984; Satishchandaran *et al.*, 1993), *Saccharomyces cerevisiae* (Thomas & Surdin-Kerjan, 1987; Thomas *et al.*, 1988), *Arabidopsis thaliana* (Peleman *et al.*, 1989a,b), *Petroselinum crispum* (Kawalleck *et al.*, 1992), rat liver (Horikawa *et al.*, 1989), rat kidney (Horikawa *et al.*, 1990), human liver (Horikawa & Tsukada, 1991), human kidney (Horikawa & Tsukada, 1993), mouse liver (Sakata *et al.*, 1993), poplar (Vandoorsselaere *et al.*, 1993), and the leaf of *Dianthus caryophllus* (Larsen & Woodson, 1991) have been reported. These sequences were aligned by the program PILEUP (Devereux *et al.*, 1984). The sequence alignment indicates that MAT is an exceptionally well conserved enzyme through evolution. The sequences range in length from 381 to 397 amino acids. A total of 132 residues are identical in all 14 sequences, and an additional 56 residues are conservatively substituted. The greatest variability of the sequences is the ca. 15 residues at each terminus. The central 363 amino acids can be aligned with no gap larger than four residues. As described above, the residues involved in the active site are expected to be essential for the activity of MAT and thus to be highly conserved. Indeed, all these residues are conserved in the reported MAT sequences of other species. The amino acid residues located inside the tightly bound dimer are mostly conserved whereas the amino acid residues on the outside surface of the dimer are less conserved, suggesting that the formation of the dimer is important for all MATs. Sequencing data and this X-ray study indicate that MATs from various species assume quite similar three-dimensional

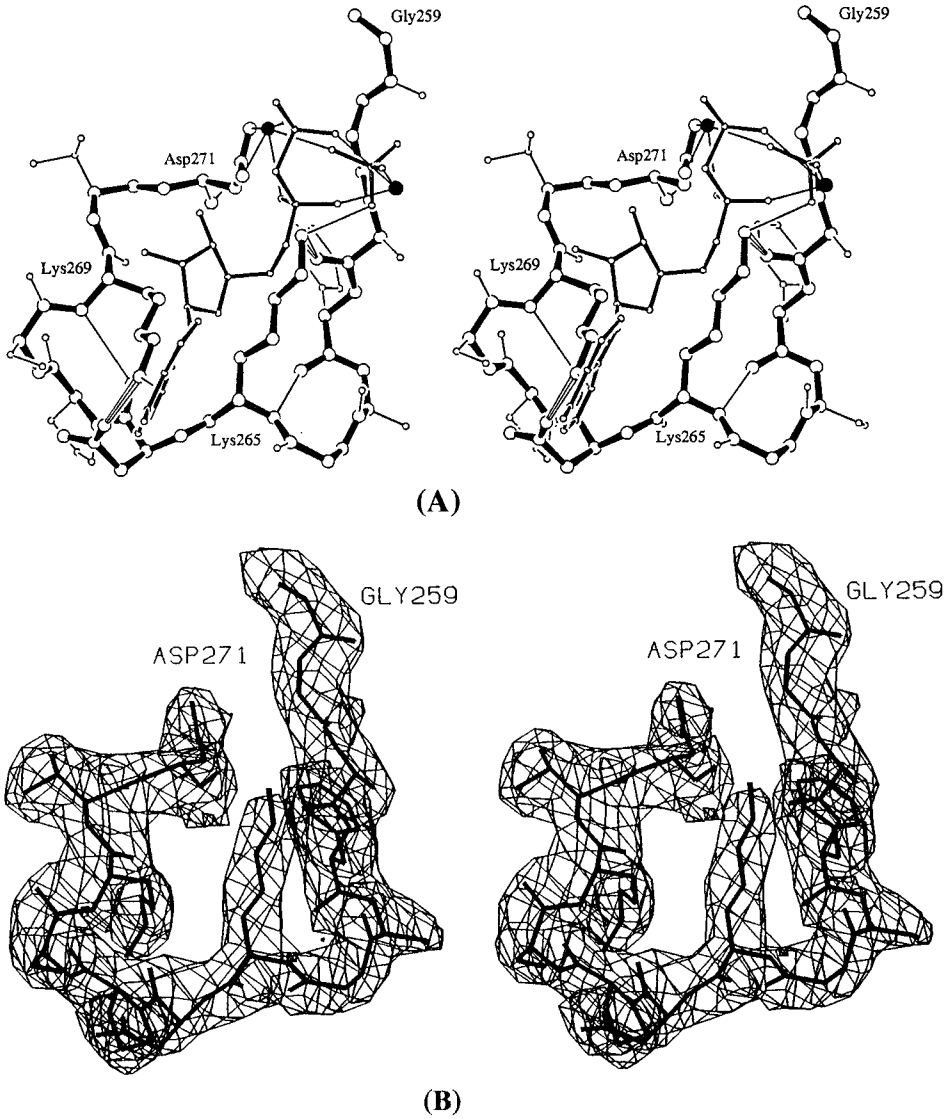

FIGURE 5: (A) A unique P-loop-like sequence and its vicinity containing two consecutive 18-atom cyclic structures (^{259}GGAFS-GKDPSKVD^{271}). ADP, P_i, and Mg^{2+} ions (solid circle) are superimposed. The backbone of the peptide and the side chains forming the 18-membered ring are indicated by thick solid bonds, whereas the other side chains are illustrated with thin bonds with small circles. Two lysines (Lys^{265} and Lys^{269}) involved in hydrogen bonds are indicated by thick three-line bonds, while the other hydrogen and coordinate bonds are shown by thin lines. (B) ($2F_o - F_c$) electron density map in the region of the P-loop-like sequence. The contours are drawn at a 1.5σ level.

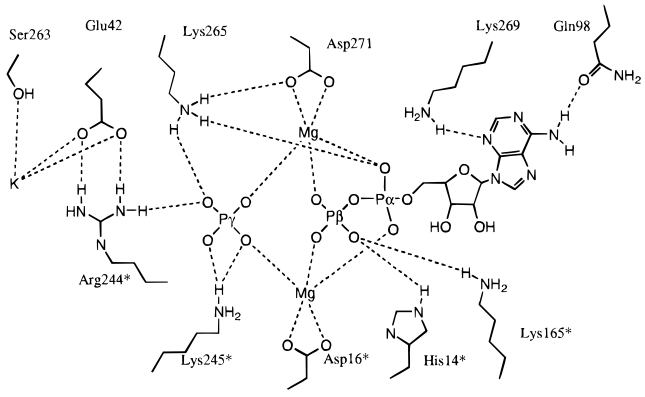

FIGURE 6: Schematic diagrams of interactions of ADP, P_i, and metal ions in the active site. The possible polar interactions (hydrogen bonds and coordinate bonds) are indicated by dashed lines.

structures including the active site geometry. Therefore, the central features of the mechanism of the catalytic reactions are probably identical in the enzymes from a wide range of organisms, despite wide differences in K_M values (Tabor & Tabor, 1984; Kotb & Geller, 1993).

Possible Enzymatic Mechanisms of MAT. The reactions catalyzed by MAT proceed without any covalent enzyme−substrate intermediates, with the initial step being reaction of L-methionine and ATP to yield AdoMet and tripolyphosphate. The AdoMet-forming reaction was found by stereochemical and kinetic isotope studies to occur as an S_N2 reaction with direct attack of the sulfur of methionine on the C5′ atom of ATP (Parry & Minta, 1982; Markham *et al.*, 1987).

On the basis of the crystal structures described here, a possible catalytic reaction mechanism of the formation of AdoMet can be proposed. In the MAT−ADP structure, the diphosphate moiety of ADP interacts extensively with the enzyme. Thus, it is quite reasonable to assume that the methionine molecule will bind near the fixed triphosphate moiety of ATP at an as yet unknown site in order to allow the catalytic reaction to take place. As shown in Figure 7, the ATP molecule apparently approaches the active site with

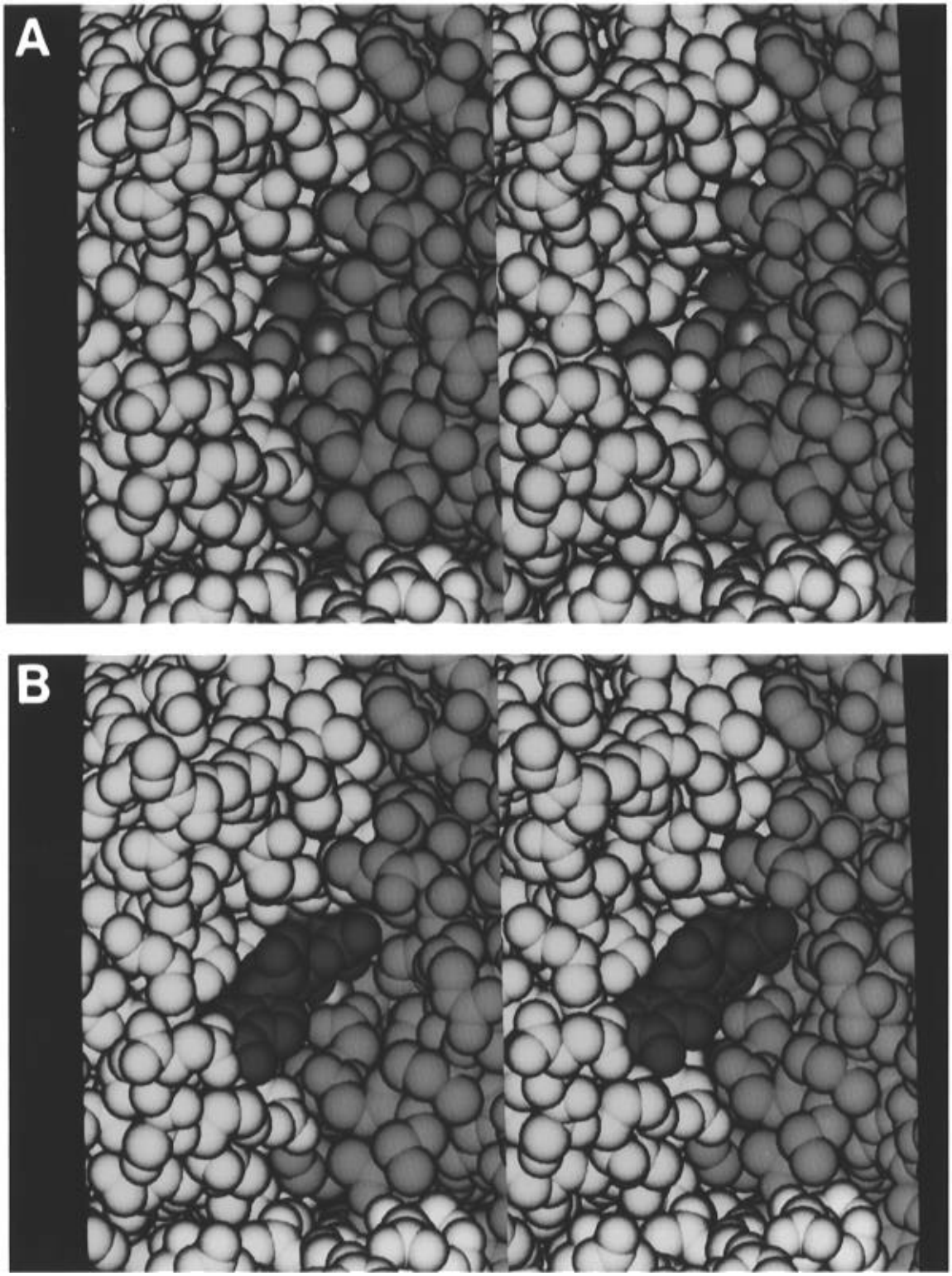

FIGURE 7: Space-filling representation showing an active site between the subunits. The flexible loops are not included in this view. (A) The active site with Mg^{2+} and K^+ ions showing a deep cleft between the two subunits. The K^+ ion in the bottom of the cleft is located at the center of the dimer and on the crystallographic 2-fold axis, and this K^+ ion appears to play a role in forming the tightly bound dimer. (B) The active site with ADP, P_i, Mg^{2+}, and K^+ ions showing a well-fitted ADP and P_i in the cleft.

the triphosphate group pointed into the wide open cleft. The triphosphate group penetrates deep inside of the cleft and is fixed there with several polar interactions with the amino acid residues forming the triphosphate pocket. Then, the ammonium group (Nζ) of Lys^{269} might move to O5′ as close as 2.6 Å from 7.1 Å merely by changing the torsion angles of the side chain. In the meantime, the methionine molecule might move into the active site and approach with its $-SCH_3$ group pointed toward C5′. Lys^{269} could form a hydrogen bond with O5′ of ATP and then transfer its ammonium proton to O5′. The C5′−O5′ bond is weakened, and at the same time, the sulfur atom of the $-SCH_3$ group attacks the C5′ atom. Finally, the C5′−O5′ bond and C5′−S bonds are synchronously cleaved and formed, respectively, to produce AdoMet. EPR studies suggest that metal coordination to the nonbridging oxygens on the α-phosphoryl group is an

important catalytic device (Parry & Minta, 1982; Markham *et al.*, 1987) but the reaction could also be facilitated by protonating the bridging O5′ oxygen.

In the after hydrolysis structure of ATP to ADP and P_i, Lys^{265} is the only amino acid residue which can interact with the negatively charged amino acid residue (Asp^{271}) and the P_i in the active site. Thus, a possible enzymatic mechanism of the tripolyphosphate hydrolysis might involve the activation of a water molecule by Lys^{265} for an in-line attack on the γ-phosphate. Before the hydrolysis takes a place, the ammonium group (Nζ) of Lys^{265} might participate in hydrogen bonds with a water molecule, Oδ2 of Asp^{271}, and the bridging oxygen atom (O_{bridge}) between the β- and γ-phosphoryl groups. A proton of the ammonium nitrogen (Nζ) of Lys^{265} could be transferred to the O_{bridge}, and then a proton of the water molecule would move to the Lys^{265}. The activated hydroxyl ion attacks on the Pγ atom and forms a trigonal bipyramidal PO_5 intermediate. The Pγ−O bond is cleaved by completion of protonation on the oxygen atom. Lys^{245*} and Arg^{244*} which bind to the P_i ion through hydrogen bonds play a role to facilitate the release of the product (P_i) from the intermediate, PO_5. Lys^{165*} and His^{14*} interacting with the β-phosphate of ADP facilitate breakage of the Pγ−O bond. The Mg^{2+} ions bridging on the phosphates appear to be involved in the hydrolysis since lack of the divalent ions eliminates the hydrolysis activity of the enzyme (Markham *et al.*, 1980).

The proposed catalytic mechanism involves two lysines (269 and 265) as general acids. The reaction is likely to occur under a physiological pH of ∼7.0, far divorced from the normal pK_a of a lysine. Therefore, it is necessary to change dramatically the pK_a of the oxygen (O5′ and O_{bridge}) and/or the lysines during the reaction. The positively charged ammonium group (Nζ) of lysine residues can participate in hydrogen bonds with the negatively charged oxygen atoms. The pK_a of those oxygens (O5′ and O_{bridge}) might change dramatically as the negative charges develop as the C5′−O5′ and P_γ−O_{bridge} bonds break, and consequently the pK_a values of the lysines (269 and 265) are decreased. If the lysines do not participate in the catalytic reactions, then His^{14} might play a major role in the catalytic reaction of AdoMet formation since His^{14} is the only residue on the surface of the active site and its normal pK_a is near 7. In this case, however, ATP must move further deep inside of the cavity so that the O5′ atom can interact with Nϵ2 of His.[14]

CONCLUSION

The *E. coli* MAT structures in the crystals grown with the substrate ATP (and BrATP) and the product PP_i have been determined at 2.8 Å resolution. The main catalysis of MAT is the two-step reaction in which the complete triphosphate chain is cleaved from ATP as AdoMet is formed with L-methionine, and the tripolyphosphate is further hydrolyzed to PP_i and P_i before the sulfonium product (AdoMet) is released. Thus, the crystal structure of MAT grown with ATP, one of the substrates, was expected to be the ATP complex in which ATP bound in the active site of the MAT. However, the crystal structure indicated that ATP bound in the active site of the enzyme and was hydrolyzed to ADP and P_i by the enzyme. The products (ADP and P_i) were found in the active site along with the essential metal ions (K^+ and Mg^{2+}). This rather unexpected finding was first confirmed by the crystal structure of the complex with PP_i and P_i and later by an HPLC analysis. The enzyme hydrolyzed ATP to ADP and P_i in 72 h under the same conditions as the crystallization of the enzyme.

In the active site, the diphosphate moiety of ADP and P_i interacts extensively with the amino acid residues from the two subunits of the enzyme, whereas the adenine and ribose moieties have little interaction with enzyme. This interaction feature is quite consistent with the MAT catalysis. The triphosphate moiety of ATP should be necessary to interact extensively with the enzyme in order to cleave both ends of the triphosphate chain. On the other hand, the weak interactions of the adenine and ribose moieties with the enzyme should facilitate the release of the product (AdoMet) from the active site after the catalytic reaction. The adenine ring of ATP is apparently recognized by forming a hydrogen bond with its N6 amino group to the carbonyl oxygen of Gln^{98}, which is the only hydrogen bond acceptor on the surface of the adenine pocket. Since ADP and P_i were found in the active site, the tripolyphosphate cleaved from ATP should be hydrolyzed between β- and γ-phosphates to produce PP_i and P_i when the normal catalysis takes place in the active site.

All amino acid residues involved in the active site are found to be conserved in the 14 reported sequences of MAT from a wide range of organisms. Thus the structure determined in this study can be utilized as a model for other members of the MAT family. On the basis of the crystal structures, the catalytic reaction mechanisms of AdoMet formation and hydrolysis of tripolyphosphate can be proposed. For AdoMet formation, the ammonium group (Nζ) of Lys^{269} might move to O5′ within a hydrogen bond distance and then transfer its ammonium proton to O5′. The C5′−O5′ bond is weakened, and at the same time, the sulfur atom of L-methionine attacks the C5′ atom. Finally, the C5′−O5′ and C5′−S bonds are synchronously cleaved and formed, respectively, to produce AdoMet. For the hydrolysis of tripolyphosphate, Lys^{265} might involve the activation of a water molecule for an in-line attack of the γ-phosphate of tripolyphosphate and transfer its ammonium proton to the bridge oxygen between β- and γ-phosphates.

ACKNOWLEDGMENT

The excellent facility and helpful cooperation provided by the NIH's Research Resource of the University of California at San Diego are gratefully acknowledged. The authors express their thanks to Professors R. L. Schowen and R. H. Hime of University of Kansas for a critical reading of the manuscript and for very valuable comments.

REFERENCES

Abad-Zapatero, C., Griffith, J. P., Sussman, J. L., & Rossmann, M. G. (1987) *J. Mol. Biol. 198*, 445−467.

Brünger, A. T. (1993) *X-PLOR 3.1: A system for X-ray crystallography and NMR*, Yale University Press, New Haven and London.

Cambillau, C., & Horjales, E. (1987) *J. Mol. Graphics 5*, 174.

Cantoni, G. L. (1953) *J. Biol. Chem. 204*, 403−416.

Devereux, J., Haeberli, P., & Smithies, O. (1984) *Nucleic Acids Res. 12*, 387−395.

Horikawa, S., & Tsukada, K. (1991) *Biochem. Int. 25*, 81−90.

Horikawa, S., & Tsukada, K. (1993) *FEBS Lett. 312*, 37−41.

Horikawa, S., Ishikawa, M., Ozasa, H., & Tsukada, K. (1989) *Eur. J. Biochem. 184*, 497−501.
Horikawa, S., Sasuga, J., Shimizu, K., Ozasa, H., & Tsukada, K. (1990) *J. Biol. Chem. 265*, 13683−13686.
Jones, T. A. (1985) *Methods Enzymol. 115*, 157−171.
Kawalleck, P., Plesch, G., Hahlbrock, K., & Somssich, I. E. (1992) *Proc. Natl. Acad. Sci. U.S.A. 89*, 4713−4717.
Koshland, D. E., Jr. (1988) *Biochemistry 27*, 5829−5834.
Kotb, M., & Geller, A. M. (1993) *Pharmacol. Ther. 59*, 125−143.
Larsen, P. B., & Woodson, W. R. (1991) *Plant Physiol. 96*, 997−999.
Larsen, T. M., Laughlin, L. T., Holden, H. M., Rayment, I., & Reed, G. H. (1994) *Biochemistry 33*, 6301−6309.
Lolis, E., Albert, T., Davenport, R. C., Rose, D., Hampton, F. C., & Petsko, G. A. (1990) *Biochemistry 29*, 6609−6618.
Ma, Q.-F., Kenyon, G. L., & Markham, G. D. (1990) *Biochemistry 29*, 1412−1416.
Markham, G. D. (1981) *J. Biol. Chem. 256*, 1903−1909.
Markham, G. D., & Satishchandran, C. (1988) *J. Biol. Chem. 263*, 8666−8670.
Markham, G. D., Hafner, E. W., Tabor, C. W., & Tabor, H. (1980) *J. Biol. Chem. 255*, 9082−9092.
Markham, G. D., Deparasis, J., & Gatmaitan, J. (1984) *J. Biol. Chem. 259*, 14505−14507.
Markham, G. D., Parkin, D. W., Mentch, F., & Schramm, V. L. (1987) *J. Biol. Chem. 262*, 5609- 5615.
Mudd, S. H., & Cantoni, G. L. (1958) *J. Biol. Chem. 231*, 481−492.
Pai, E. F., Kabsch, W., Krengel, U., Holmes, K. C., John, J., & Wittinghofer, A. (1989) *Nature 341*, 209−214.
Parry, R. J., & Minta, A. (1982) *J. Am. Chem. Soc. 104*, 871−872.
Peleman, J., Saito, K., Cottyn, B., Engler, G., Seurinck, J., Van Montagu, M., & Inze, D. (1989a) *Gene 84*, 359−369.
Peleman, J., Boerjan, W., Engler, G., Seurinck, J., Botterman, J., Alliotte, T., Van Montagu, M., & Inze, D. (1989b) *Plant Cell 1*, 81−93.
Sakata, S., Shelly, L. L., Ruppert, S., Schutz, G., & Chou, J. Y. (1993) *J. Biol. Chem. 268*, 13978−13986.
Saraste, M., Sibbald, P. R., & Wittinghofer, A. (1990) *Trends Biochem. Sci. 15*, 431−434.
Satischandran, C., Taylor, J. C., & Markham, G. D. (1993) *Mol. Microbiol. 9*, 835−846.
Sufrin, J. R., Dunn, D. A., & Marshall, G. R. (1981) *Mol. Pharmcol. 19*, 307−313.
Sufrin, J. R., Lombardini, J. B., & Alks, V. (1993) *Biochim. Biophys. Acta 1202*, 87−91.
Tabor, C. W., & Tabor, H. (1984) *Adv. Enzymol. 56*, 251−282.
Takusagawa, F. (1992) *J. Appl. Crystallogr. 25*, 26−30.
Takusagawa, F., Kamitori, S., Misaki, S., & Markham, G. D. (1995) *J. Biol. Chem. 271*, 136−147.
Tanaka, I., Yao, M., Suzuki, M., Hikichi, K., Matsumoto, T., Kozasa, M., & Katayama, C. (1990) *J. Appl. Crystallogr. 23*, 334−339.
Thomas, D., & Surdin-Kerjan, Y. (1987) *J. Biol. Chem. 262*, 16704−16709.
Thomas, D., Rothstein, R., Rosenberg, N., & Surdin-Kerjan, Y. (1988) *Mol. Cell. Biol. 8*, 5132−5139.
Vandoorsselaere, J., Gielen, J., Van Montagu, M., & Inzè, D. (1993) *Plant Physiol. 102*, 1365−1366.
Xuong, Ng. H., Nielsen, C., Hamlin, R., & Anderson, D. (1985) *J. Appl. Crystallogr. 18*, 342−350.
Zhang, C., Markham, G. D., & Lobrutto, R. (1993) *Biochemistry 32*, 9866−9873.

BI952604Z